SACLANTCEN REPORT
serial no.: SR-143

SACLANT UNDERSEA
RESEARCH CENTRE

REPORT

Acoustic source-level measurements for a variety of merchant ships

P. Scrimger and
R.M. Heitmeyer

July 1988

Page count for SR-143
(excluding covers)

Pages	Total
i–iv	4
1–27	27
	31

SACLANT Undersea Research Centre
Viale San Bartolomeo 400
19026 San Bartolomeo (SP), Italy

tel: 0187 540 111
telex: 271148 SACENT I

NORTH ATLANTIC TREATY ORGANIZATION

Report no. changed (Mar 2006): SR-143-UU

SACLANTCEN SR-143

Acoustic source-level measurements for a variety of merchant ships

P. Scrimger and R.M. Heitmeyer

The content of this document pertains to work performed under Project 21 of the SACLANTCEN Programme of Work. The document has been approved for release by The Director, SACLANTCEN.

Peter C. Wille
Director

intentionally blank page

Acoustic source-level measurements for a variety of merchant ships

P. Scrimger and R.M. Heitmeyer

Abstract: This report describes a set of 50 source spectra obtained from merchant ships of opportunity near Genova, Italy. These spectra were obtained from radiated-noise spectra measured on a towed array and a transmission-loss spectrum computed from a parabolic equation model. The characteristics of the ships are presented for the 32 spectra where the ship name was determined. The sub-sample of 36 spectra with known ship type is characterized in terms of three ship classes – passenger/ferries, cargo ships and tankers. It is seen that the ship class percentages for this sub-sample differ significantly from the ship class percentages for either a Mediterranean population or a World population. The source spectra are characterized in terms of the mean source spectrum and source-level histograms computed over three frequency bands. The mean spectrum is comparable in level and shape to a spectrum computed from a well-known empirical model. The source-level histograms for the low-frequency and the medium-frequency bands are approximately gaussian with standard deviations of 5 dB and 5.5 dB respectively. The histogram for the high-frequency band is skewed somewhat towards the low source-level values with a standard deviation of 6.8 dB. Finally, it is seen that the source spectra for the three ship classes have comparable means and comparable standard deviations. From this result we conjecture that both the mean spectrum and the source-level histograms are representative of the shipping in other regions with different ship class percentages.

Keywords: acoustics ○ shipping ○ ship-radiated noise ○ source levels

Contents

Acknowledgement: The authors would like thank Miss B. Sotirin who was responsible for a number of the acoustic computations and Dr. R. Hollett, Mr. A. Trangeled and Mr. E. Baglioni for their contributions to the software development and the data acquisition.

1. Introduction

In November 1985, the radiated-noise spectra for 50 merchant ships were measured over a frequency band of 70 to 700 Hz using a towed array in a region located south of the port of Genova, Italy. These spectra were converted to source spectra through the addition of a transmission-loss spectrum obtained from a parabolic equation acoustic model. The results were collected together in a database that consists of the 50 individual source spectra along with the characteristics of the ships whose identity could be determined. Finally, the characteristics of the source spectra were summarized in terms of the mean source spectrum and histograms of the source level relative to the mean for different frequency bands. These statistics constitute the source-level description required by a number of ambient noise models that compute the noise observed at a site due to the aggregate of the ships in the region.

2. Methodology

The source spectra were each obtained as the sum of a measured radiated-noise spectrum and a computed transmission-loss spectrum. The radiated-noise spectra were measured on ships of opportunity over a 6-day period using a horizontal array towed by the R/V *Maria Paolina G.* in the 25 n.mi × 40 n.mi area indicated in Fig. 1. Within this area, the bottom depth decreases from about 200 m to over 2000 m as the continental shelf falls to the abyssal plain. The detailed bathymetry in the region is further complicated by a number of submarine canyons which cut deep grooves in the continental shelf. The approximate locations of these canyons together with bottom composition estimates for the region are described in Appendix B.

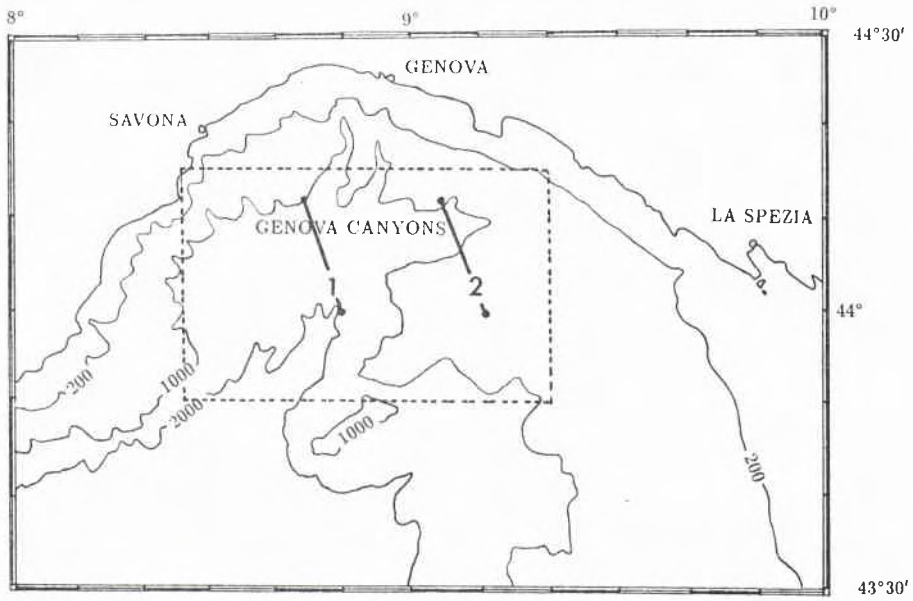

Fig. 1. The operating area.

The bottom parameters needed for the acoustic model were inferred from transmission-loss data that was measured along the two tracks shown in Fig. 1. This data was acquired on the endfire beam of the towed array from a multi-tone source deployed at a depth of 6 m by the T/B *Manning* at the northernmost point of each track. In a subsequent analysis, the transmission-loss measurements were compared with the transmission loss computed from the parabolic equation model using sound-speed

and bottom-depth profiles measured along the tracks and a wide range of bottom parameters. It was found that essentially the same set of bottom parameters resulted in a good fit to the transmission-loss measurements for both tracks. This set of bottom parameters is given in Appendix B.

The radiated-noise spectrum for each ship $\mathrm{RL}(f)$ was measured at the output of a conventional frequency-domain beamformer as the array was towed along a track in the operating area at a nominal speed of 5 kn. This spectrum was in turn obtained as a decibel average of a set of individual radiated-noise spectra $\mathrm{RL}_k(f)$ where each $\mathrm{RL}_k(f)$ was computed as an 83 s power average. During the 83 s period, the range to the ship typically varied by several tenths of a nautical mile and there was virtually no change in the bearing to the ship relative to the beamwidth. The total averaging period for the averaged radiated-noise spectrum $\mathrm{RL}(f)$ was typically about 11 min during which the range to the ship would usually vary by a few nautical miles and there was often a significant change in the ships bearing. Finally, the individual radiated-noise spectra $\mathrm{RL}_k(f)$ were themselves obtained by tracking the ship in a time series of 'frequency-angle noise surfaces'. These noise surfaces were formed from the beam spectra for a set of 128 beams distributed over the full 180° beam steering angle sector. The individual radiated-noise spectra were obtained from these noise surfaces by identifying the steering angle which had the maximum response in the target-ship direction. An example of a noise-surface time series for a particular ship and a description of the procedure used to obtain the individual radiated-noise spectra is presented in Appendix A. The spatial shading used in the beamformer was such that the broadside beamwidth ranged from about 2.8° at 700 Hz to about 34° at 62.5 Hz. All spectra were estimated for an analysis bandwidth of 3.75 Hz and a frequency-line spacing of 2.5 Hz.

The data acquisition procedures were organized into two operational modes – a ship-selection mode and a data-recording mode. In the ship-selection mode, the array was towed along some search track in the operating area while the ship traffic in the region was monitored on both the noise-surface display and a radar display. As soon as a potential target ship was identified, the ship track information from the radar display was used to select a new course for the array-tow ship. This course was chosen to orient the array so that the radiated-noise spectrum from the target ship was well separated in steering angle from the noise contributions from the other ships in the region on the noise-surface display. Once it was determined that the target ship noise contribution was clearly visible in the noise-surface display, the data-recording mode began. In this mode, the noise-surface time series was recorded on magnetic tape while the noise-surface display was monitored to identify those surfaces where the target ship spectrum was not corrupted by the contributions of interfering sources. At the same time, the range and bearing to the target ship was determined from the radar display in time coincidence with the noise-surface measurements. This data was recorded along with the tow-ship navigational data to provide for the reconstruction of the tow ship and the target-ship tracks. In addition, an attempt was made to contact the target ship by radio to establish its identity.

After the data recording was completed, a new ship course was selected and the ship-selection mode for the next ship began. Note that by virtue of these procedures, the set of radiated-noise spectra were obtained for different tow-ship/target-ship track configurations and different target-ship aspect angles.

The transmission-loss spectrum $\mathrm{TL}(f)$ was obtained using the acoustic model to first compute the transmission-loss spectrum as a function of range $\mathrm{TL}(f, r)$ and then averaging $\mathrm{TL}(f, r)$ over the range interval associated with the corresponding radiated-noise spectrum $\mathrm{RL}(f)$. All transmission-loss computations were done for a source depth of 6 m using a measured sound-speed profile and the bottom composition parameters given in Appendix B. To determine the bottom-depth profiles for the acoustic model, a set of approximate bottom-depth profiles was estimated for the 50 ships using the measured tow-ship/target-ship tracks and bottom depth data. The transmission-loss function $\mathrm{TL}(f, r)$ was then computed for a number of bottom-depth profiles from this set. From an inspection of these functions and a consideration of the range intervals associated with the different tow-ship/target-ship track configurations, a set of six generic bottom-depth profiles was selected to represent the full set of profiles. The transmission-loss function $\mathrm{TL}(f, r)$ for each ship was then computed using the generic bottom depth profile that most closely approximated the actual profile. Further details on the acoustic modelling are contained in Appendix B along with the six generic bottom-depth profiles and the resulting transmission-loss functions.

3. The source-spectrum equation

The source spectrum for each ship $\mathrm{SL}(f)$ was determined from the averaged radiated-noise spectrum for that ship and the corresponding transmission-loss spectrum according to

$$\mathrm{SL}(f) = \mathrm{RL}(f) + \mathrm{TL}(f), \tag{1}$$

where

$$\mathrm{RL}(f) = \frac{1}{K}\sum_{k=1}^{K} \mathrm{RL}_k(f), \tag{2a}$$

$$\mathrm{TL}(f) = \frac{1}{K}\sum_{k=1}^{K} \mathrm{TL}(f, r_k), \tag{2b}$$

K is the number of individual radiated-noise spectra, and $\mathrm{TL}(f, r_k)$ is the average of $\mathrm{TL}(f, r)$ over the range interval associated with the individual radiated-noise spectrum. All spectra are expressed in $\mathrm{dB}/\mu\mathrm{Pa}/\mathrm{Hz}$ and the source spectrum and the transmission-loss spectrum are referred to a 1 m distance from the source. The analysis bandwidth associated with $\mathrm{RL}(f)$ and hence with $\mathrm{SL}(f)$ is 3.5 Hz. The spectra are described at 253 discrete frequencies ranging from 70 Hz to 700 Hz in 2.5 Hz increments.

The implications of the methodology summarized in Eq. (1) are threefold. First, by virtue of the source depth used to compute the transmission-loss spectrum $\mathrm{SL}(f)$ describes the noise radiated by the ship as a monopole source located at a depth of 6 m. This depth was chosen to be representative of a class of merchant ships. Other choices for the source depth, say the propeller depth, could yield source-spectra that differ from $\mathrm{SL}(f)$. Secondly, since the radiated-noise spectra were measured over a limited range of aspect angles, there is a potential dependence on the ships radiation pattern that is not accounted for in $\mathrm{SL}(f)$. Finally, since $\mathrm{RL}(f)$ was obtained as a time-average, $\mathrm{SL}(f)$ itself must be considered as a time-averaged source spectrum. In this regard, we note that in all instances the ships measured appeared to be travelling at their normal speed along a fixed course during the time of the measurement.

4. The ship characteristics

Out of the total sample of 50 spectra, it was possible to determine the ship name for 32 of those spectra and the ship type for an additional four spectra. Most of the 32 ship names were identified through a radio contact made during the time of the data acquisition for the ship. On some of the occasions where a radio contact could not be established, the ship name was unambiguously determined from ship departure time and destination data supplied by the Genova Port authorities. The four ship-type identifications were made visually during the time of the data acquisition. We use this information to summarize the characteristics of the ships in the Genova sample and to compare the ship-type composition of that sample with ship-type compositions for a World population, a Mediterranean population and an Italian population. In Sect. 6 we consider the implications of this comparison on the applicability of the Genova source-spectrum statistics to regions with different ship-type compositions.

The ship characteristics for the 32 ships are listed in Table 1 along with the ship type for the 4 ships where only a visual contact was possible. The ship characteristics were obtained from *Jane's Merchant Ships* [1]. These characteristics consist of the ships identification number, name, flag, type, gross tonnage, length, draught, speed and number of propeller screws. The ship type is abbreviated in accordance with *Jane's* convention:

P – Passenger ship

RoC – Roll-on/roll-off Cargo ship

RoPCF – Roll-on/roll-off Passenger Car Ferry

Tk – Oil and oil products Tanker

C/HL – Cargo ship (Heavy Lift)

RoPF – Roll-on/roll-off Passenger Ferry

C – Cargo ship

Tk/Ch – Oil and oil products Tanker/Chemical tanker

Any ship not so identified, i.e. ships labelled 'Tanker', 'Cargo' etc., were visual identifications only and not found in *Jane's*. The GRT (tons) column gives the gross ship tonnage defined as the total 'volume' of enclosed space (100 cu ft=1 t). The ship length and ship draught are given in meters and the ship speed is in knots. The ship speed is the normal operating speed as listed in *Jane's*, these speeds agreed well with those values estimated from the radar during data acquisition (normally

Table 1
The ship characteristics

SHIP NO.	JANES ID.	SHIP NAME	FLAG	SHIP TYPE	GRT (TONS)	LENGTH (M)	DRAUGHT (M)	SPEED (KTS)	NO. SCREWS
1				-					
2	16930	HABIB	TUNISIA	P/RoC	11200	143	6.0	22.	2
3	33471	CLODIA	ITALY	RoPCF	10500	136	5.9	20.	2
4				-					
5				-					
6	33472	NOMENTANA	ITALY	RoPCF	10500	136	5.9	20.	2
7				-					
8	32557	PETRARCA	ITALY	RoPCF	6500	131	5.6	20.5	2
9	22382	STAFFETTA TIRRENICA	ITALY	RoC	4700	141	5.9	19.	2
10	33471	CLODIA	ITALY	RoPCF	10500	136	5.9	20.	2
11	94521	AMIRA	FRANCE	RoC	3500	133	6.6	18.5	1
12	69690	PAPANIKOLIS	CYPRUS	Tk	41200	238	12.8	16.	1
13	00969	STAFFETTA LIGURE	ITALY	RoC	6900	148	6.3	20.	2
14	51211	HIMALAYA	JAPAN	C/HL	16000	166	10.4	16.	1
15	33474	AURELIA	ITALY	RoPCF	10500	136	5.9	20.	2
16	20355	LEV TOLSTOY	USSR	RoPF	9900	134	5.3		2
17	16421	J.J.SISTER	SPAIN	RoPF	9100	141	6.4	23.5	2
18				-					
19				-					
20	16391	DANAE	GREECE	P	11700	162	10.0	17.	2
21	65760	ANTEA	ITALY	Tk	17600	172	10.7	15.5	1
22	38732	NIAGARA	ITALY	Tk	22000	208	11.6	16.5	1
23	49496/2	RUBEN M. VILLENA	HUNGARY	C	11800	162	9.2	18.	1
24	33471	CLODIA	ITALY	RoPCF	10500	136	5.9	20.	2
25	33476	FLAMINIA	ITALY	RoPCF	10500	136	5.9	20.	2
26				-					
27	-	VALGARDENA		TANKER					
28				-					
29	-	DONNA BRUNA		CARGO	3000				
30	54150	LADY AUGUSTA	ITALY	Tk/Ch	1800	87	5.4	13.	1
31				-					
32	66197	AGIP GELA	ITALY	Tk	18000	171	10.9	16.5	1
33	-	BRAZIL GLORY	BRAZIL	TANKER	54095				
34				CARGO					
35				-					
36	00969/1	STAFFETTA IONICA	ITALY	RoC	6900	148	6.3	20.	2
37	32556	PASCOLI	ITALY	RoPCF	6500	131	5.6	20.5	2
38	76730	FRECCIA BLU	ITALY	RoC	5700	164	6.0	21.	2
39	32557	PETRARCA	ITALY	RoPCF	6500	131	5.6	20.5	2
40				-					
41	33473	EMILIA	ITALY	RoPCF	10500	136	5.9	20.	2
42				CARGO					
43				CARGO		150			
44				-					
45				-					
46	60126	SITHONIA	JAPAN	C	8000	142	9.1	14.5	1
47				-					
48				TANKER	3000				
49	49640	CALA MEDITERRANEA	PANAMA	C	8400	144	8.3	18.	1
50	72758	EURO FREIGHTER	FINLAND	C	500	78	4.1	13.	1

within about 20%). As seen in the last column of Table 1, most of the ships identified have twin screw propulsion systems.

The ship-type comparison was obtained by grouping the 36 ship types in the Genova sub-sample into three classes: tankers (Tk, Tk/Ch), cargo ships (RoC, C/HL, C) and passenger/ferry ships (P, RoPCF, RoPF). These ship classes comprise 45% of the world shipping and 75% of the world shipping if fishing boats, pleasure boats and the various specialized ships such as icebreakers, research vessels, tugs and dredgers

are excluded. The total number of ships in these classes for the World, the Mediterranean and the Italian populations were obtained from *Lloyd's Register of Shipping, Statistical Tables* [2]. The ship-class totals for the Mediterranean population were determined as the sum of the number of ships registered in each of the countries bordering on the Mediterranean Sea for the appropriate ship class.

Table 2
Ship class totals for the World, Mediterranean and Genova populations

Class	Ship type	World	Mediterranean	Genova
1(a)	oil tankers	7021	1059	7
1(b)	chemical tankers	774	76	1
2	cargo ships	22242	4573	14
3(a)	ferries/passenger	3526	813	13
3(b)	passenger/cargo	245	21	1
		33808	6542	36

Table 3
Mediterranean shipping population by country

Class	Ship type	Greece	Italy	Spain	France	Others	Total
1(a)	oil tankers	441	247	104	89	178	1059
1(b)	chemical tankers	2	30	11	7	26	76
2	cargo ships	1634	365	515	196	1863	4573
3(a)	ferries/passenger	271	221	48	53	220	813
3(b)	passenger/cargo	7	0	1	1	12	21
		2355	863	679	346	2299	6542

Figure 2 shows the percentage of the ships in each ship class for the World population, the Mediterranean population and the Genova sub-sample. These ship-class percentages are obtained from the corresponding ship-class totals listed in Table 2. As seen in the figure, the composition of the World population is comparable to that

of the Mediterranean population with each consisting of about 20% tankers, nearly 70% cargo ships and slightly more than 10% passenger/ferry ships. The composition of the Genova sub-sample, however, differs significantly from that of the others with a much larger percentage of passenger/ferries and a lower percentage of cargo ships.

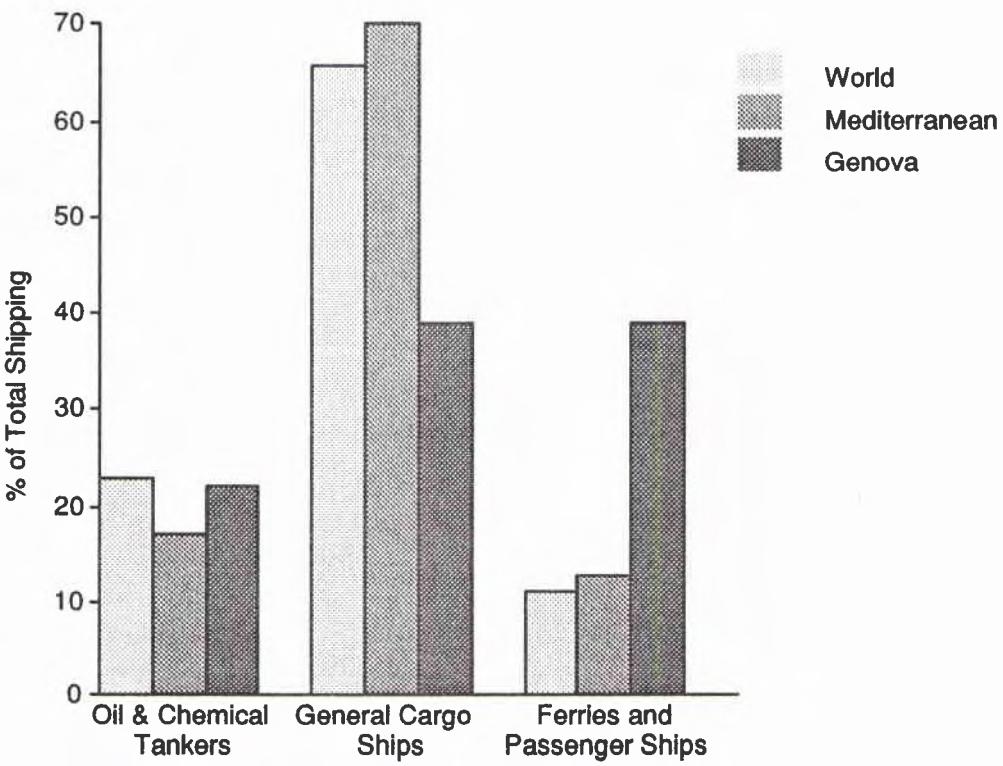

Fig. 2. Ship-class percentages for the World, the Mediterranean and the Genova sub-sample populations.

An explanation for the differences in the ship-type composition can be found in the breakdown of the Mediterranean ship-type composition by country shown in Table 3. The first four columns of this table contain the ship-class totals for the four major shipping countries in the Mediterranean; the fifth column, labelled 'Others', contains the sum of the ship-class totals for the remaining Mediterranean countries. As seen in the bottom row of the table, Italy with 863 ships is second only to Greece (2355 ships) in the total number of registered ships. Nevertheless, Italy accounts for only about 12% of the total Mediterranean shipping population and hence, the Italian shipping is not the major determinant of the Mediterranean ship-type composition. Furthermore, Italy has a larger proportion of passenger/ferries

and a smaller proportion of cargo ships than the Mediterranean shipping. This can be seen by noting that with 221 passenger/ferries, Italy is a very close second to Greece which has 278 passenger/ferries; whereas, with 365 cargo ships, Italy is well behind Greece (1634 cargo ships) and Spain (515 cargo ships). This difference is consistent with the Genova sub-sample where the number of passenger/ferries is disproportionally high and the number of cargo ships is disproportionally small. We note in passing that Italy has the largest number of chemical tankers with 30, or approximately 3.5% of the Italian total; one of these chemical tankers was observed (*Lady Augusta*) in the Genova sub-sample.

The Italian ship-class percentages are shown quantitatively in Fig. 3 along with the ship-class percentages for the Genova sub-sample. This figure together with Fig. 2 indicates that the composition of the Genova sub-sample is more representative of the Italian population than either the World population or the Mediterranean population.

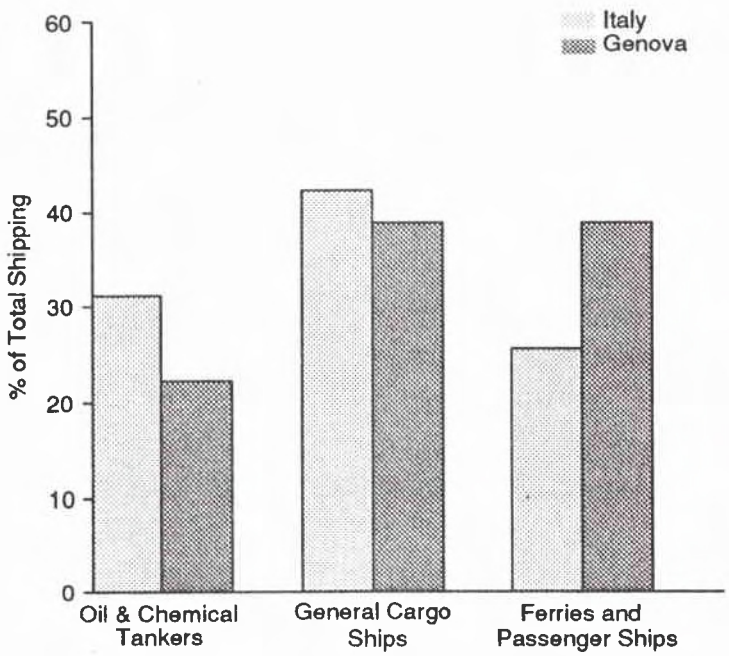

Fig. 3. Ship-class percentages for the Italian and the Genova sub-sample populations.

5. The source spectra

In this section we describe the general characteristics of the measured source spectra and present the mean source spectrum and three relative source-level histograms obtained from those source spectra. The mean source spectrum is compared with a predicted spectrum obtained from the empirical model of Ross [3], and the source-level histograms are compared with a gaussian probability density. Finally we compare the published source spectra for three other ships with those from the Genova sample.

The full set of 50 source spectra are plotted in Fig. 4 along with the mean source spectrum and the predicted source spectrum. The mean source spectrum was computed as the decibel average of the individual source spectra. The predicted spectrum was obtained using the 'POST-WWII' spectrum of Fig. 8.20 in [3]. This spectrum represents an average spectrum for a number of freighters and tankers expressed relative to an overall level L_s'. The overall level L_s' was computed from Eq. (8.35) of [3]. This equation determines L_s' in terms of the number of propeller blades B and the propeller tip speed U_t according to

$$L_s' \approx 175 + 60 \log (U_t/25 \text{ m/s}) + 10 \log \left(\tfrac{1}{4}B\right) . \tag{3}$$

The level L_s' was computed for four propeller blades ($B = 4$) and a propeller tip speed of 37.5 m/s. This tip speed represents the mid-point of the common propeller tip speeds suggested by Ross.

As can be seen in Fig. 4, the individual source spectra differ significantly from one another in both shape and level. For frequencies up to about 150 Hz, all of the spectra decrease with frequency at roughly the same rate. For larger frequencies, many of the spectra continue to decrease with frequency although at significantly different rates; other spectra actually show an increase in level at the higher frequencies. This difference in shape gives rise to a difference in the total range of source levels at different frequencies. This range increases with frequency from about 24 dB at the lower frequencies to about 30 dB at the higher frequencies. Note also that, in spite of the large 3.5 Hz analysis bandwidth, there are strong spectral lines evident in a number of the spectra. Most of these lines fall within two frequency bands: 210 Hz to 220 Hz and 350 Hz to 360 Hz. The lines in the lower-frequency band are from the spectra of three of the eight ships in the tanker class, the *Papanikolis*, the *Agip gela* and the *Brazil glory*. The lines in the higher frequency band (350–360 Hz) are from the spectra of seven of the fourteen spectra in the passenger/ferry class. Three of these seven spectra were measured at different times from the same ship, the passenger car ferry *Clodia*; the remaining four spectra are from her sister ships, the *Nomentana*, the *Flaminia*, the *Pascoli* and the *Emilia*.

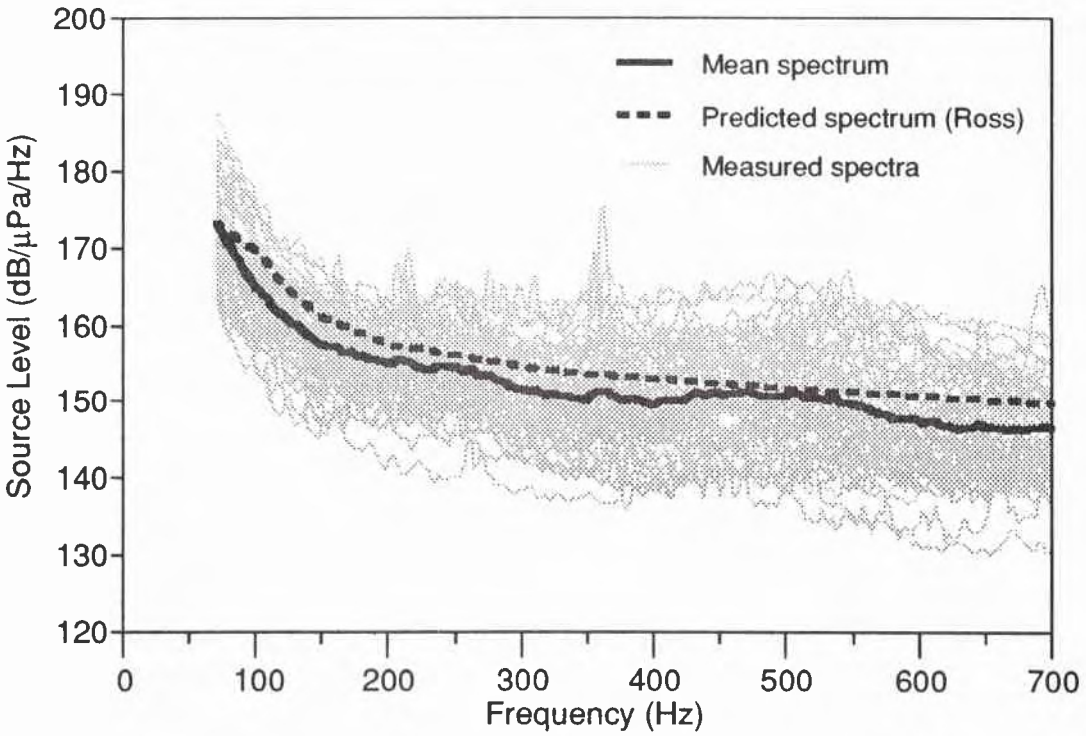

Fig. 4. The 50 individual source spectra, the mean source spectrum and a predicted source spectrum.

The mean source spectrum in Fig. 4 shows a fairly strong decrease with frequency up to about 170 Hz (about −12 dB/octave) followed by a more gradual decrease over the rest of the frequency band (about −3 dB/octave). Note, however, that there is a slight increase between about 450 Hz and 550 Hz that results from the contributions of the individual spectra with high spectrum levels in this frequency band. Furthermore, note that the mean spectrum is only about 2 to 3 dB lower than the predicted spectrum over most of the frequency band. The exceptions occur between 450 Hz and 550 Hz where there is no increase in level in the predicted spectrum and for frequencies less than about 100 Hz where the slope of the predicted spectrum is only about −7 dB per octave.

The source-level histograms describe the variation in the source level for the full set of spectra relative to the mean source level. These histograms have been estimated over three frequency bands, a low-frequency band (70–200 Hz), a medium-frequency band (240–340 Hz) and a high-frequency band (400–700 Hz). The results are shown in Fig. 5 along with the standard deviation of the source-level, σ, and a gaussian probability density determined for a standard deviation of σ and a relative source-

level of zero. The histogram for each frequency band was estimated by first computing the decibel difference between the source-level and the mean spectrum for all spectra at each frequency in the band and then forming the histogram from the resulting set of differences. The frequency bands were chosen through a qualitative assessment of the frequency intervals where the relative source-level appeared to be distributed over the same range of values. Note that these frequency bands exclude the strong spectral lines seen in Fig. 4.

As expected from the plots of the individual spectra in Fig. 4, the high-frequency source-level histogram shows a greater spread than the low-frequency histogram. This is evidenced by the increase in the standard deviation from 5 dB for the lower-frequency band to 6.8 dB for the high-frequency band. Furthermore, there is some difference in the form of the histograms for the two frequency bands. For the low-frequency band the histogram is well-approximated by the gaussian probability density, whereas for the high-frequency band there is some skew towards the lower source-level values. The histogram for the medium-frequency band is similar to that of the low-frequency band with a near-gaussian form and a slightly larger standard deviation of 5.5 dB.

In the remainder of the section we compare the Genova source spectra with the source spectra of three other ships taken from the literature. Figure 6, which is taken from [3], shows the source spectrum of the passenger ship *Astrid* at a number of different speeds ranging from 9 to 18 kn. By comparison, the average speed of the ferries/passenger ship class measured in this experiment was on the order of 20 kn. The increased speed of the newer ferries and passenger vessels is expected to lead to slightly higher acoustic noise levels than the 18 kn spectrum shown in Fig. 7. A comparison of the overall source spectrum obtained for the Genova spectra to the spectrum for *Astrid* shows very good agreement throughout the full spectral band from 70.0 Hz to 700.0 Hz.

The source spectrum of the containership M/S *Jutlandia* shown in Fig. 7 is taken from a consulting engineering report prepared for Greenland Fisheries Investigations, based in Copenhagen, Denmark [4]. This ship is 274 m long with triple screws and capable of a maximum speed of 30 kn. The spectrum shown in the figure was measured as the ship was sailing at a constant speed of 27 kn with all engines running at almost full power. The three measured curves were estimates of the source level for measurements taken at 220, 460 and 1850 m from the ship. The dotted line shown is the predicted source level calculated according to Ross using the WWII spectrum. It is of interest to note that even though this is a much larger ship travelling considerably faster than those in the Genova sample, the spectrum is not much different from the mean spectrum of Fig. 4.

The source spectrum of a medium-sized oil tanker (24000 DWT) shown in Fig. 8 was taken from [5]. This ship is 148 m in length and is typical of the type of tanker found in the Genova sample. The spectra shown in the figure were measured with a

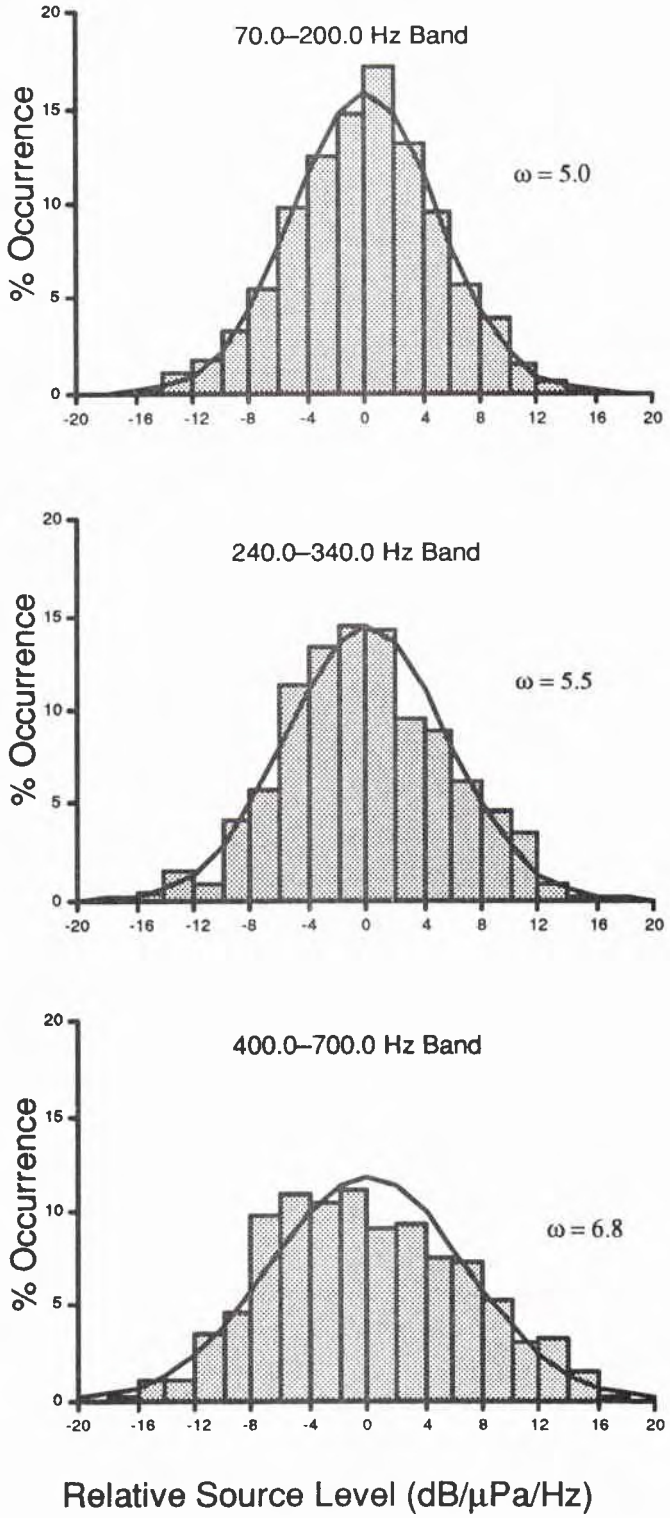

Fig. 5. The relative source-level histograms.

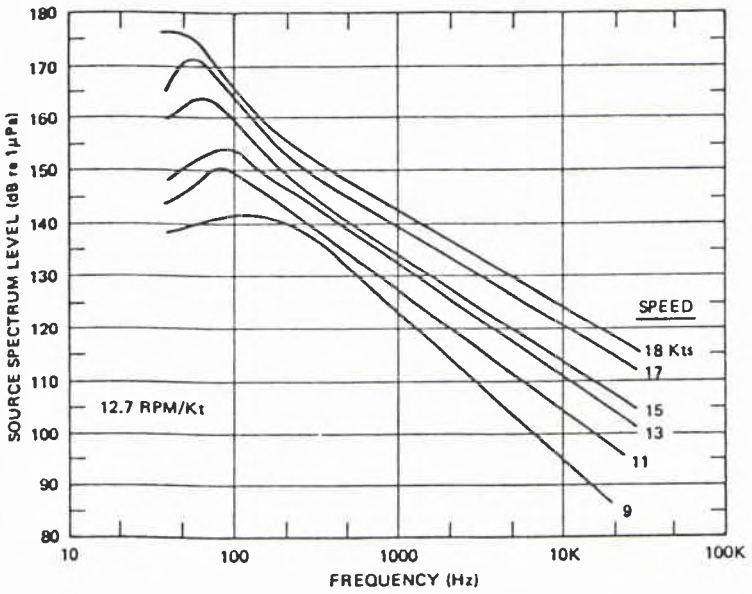

Fig. 6. Radiated noise of the passenger ship *Astrid*, as measured during WWII.

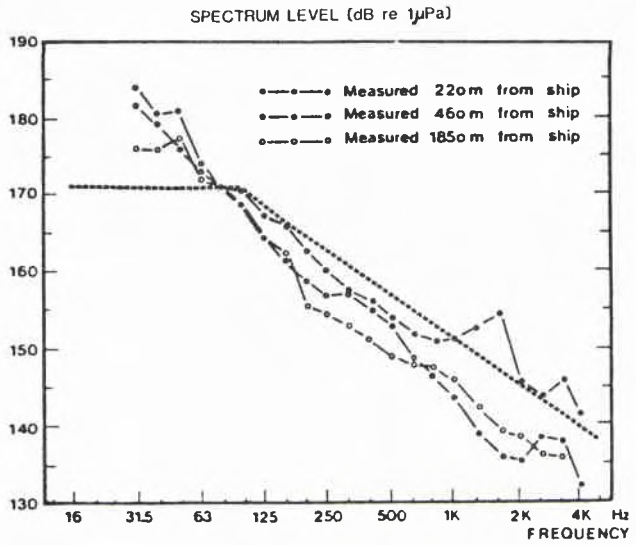

Fig. 7. Radiated noise of the container ship M/S *Jutlandia*.

hull flush-mounted hydrophone at four different ship speeds ranging from full power to half power. The design speed of this tanker was 15 kn. The source spectra shown are consistent with the type of spectra found in the Genova data. At the upper frequency of 700 Hz, the levels for this tanker range from about 130 dB to about 142 dB compared to the mean level for the Genova sample of 145 dB. The lower-frequency portion of the measured tanker spectrum shows a marked jump below about 150 Hz. In this region the tanker spectrum takes a rapid rise of about 20 dB until it peaks at approximately 50 Hz. This rise is comparable to the increase in the spectrum level for the Genova spectra of Fig. 4 which also exhibit a steep rise in this frequency region.

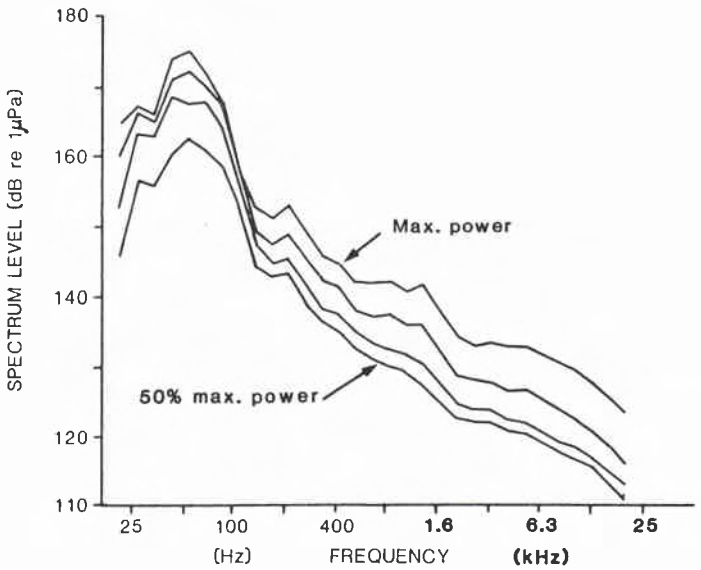

Fig. 8. Radiated noise of a medium-sized oil tanker.

6. Statistics for the three ship classes

In Sect. 4, it was seen that the ship-class percentages for the Genova sub-sample were more representative of an Italian population than either a World population or a Mediterranean population. Although the Genova sub-sample consists of only 36 of the 50 source spectra, this suggests that the source-spectrum statistics presented in the preceding section might be biased by the particular mix of ship types in the Genova sample. If this is the case, then these statistics would not be directly applicable to other regions with different ship class percentages. In this section, we address this issue by comparing statistics computed on the Genova sub-sample for the three ship classes. Because of the comparatively small number of spectra in the Genova sub-sample (8 passenger/ferries, 14 cargo ships and 14 tankers), we limit the comparison to the mean and the standard deviation.

The mean spectrum for each of the three ship classes is shown in Fig. 9. As can be seen in the figure, the three mean spectra lie within 2 dB of each other over most of the 70 Hz to 700 Hz frequency band. The only significant exception occurs between 570 Hz and 700 Hz where the mean spectrum for the tankers is about 4 dB less than the mean spectra for the passenger/ferries and the cargo ships. By way of comparison, the standard deviation for the full 50 spectrum sample increases from about 5 dB at the lower frequencies to almost 7 dB at the higher frequencies. Thus, the mean spectra for the three ship classes are essentially within one-half of a standard deviation of the full ship sample.

The standard deviation curve for each ship class is shown in Fig. 10. Each of these curves can be viewed as consisting of a slowly-varying component that changes over frequency intervals of about 100 Hz and a rapidly-varying component that changes over intervals of about 10 Hz. The rapidly-varying component results from the detailed structure of the individual spectra that make up the ship class sample as is evidenced by the fact that the variation occurs over frequency intervals that are few times the analysis bandwidth. As such, the rapidly-varying component is less representative of the standard deviation than the slowly-varying component. Consequently, we consider only the slowly-varying components of the standard deviation curves. An approximation to these components can be obtained by visually neglecting the local maxima and minima in each standard deviation curve. From these approximations it is seen that the standard deviations for the three ship classes lie within about 1.5 dB of one another over most of the frequency band. Again the most notable exception occurs for frequencies between about 570 Hz and 700 Hz where the maximum difference is about 2 dB.

The comparisons of the mean spectra and the standard deviation curves provide evidence that the source-level histograms as well as the mean spectrum for the three

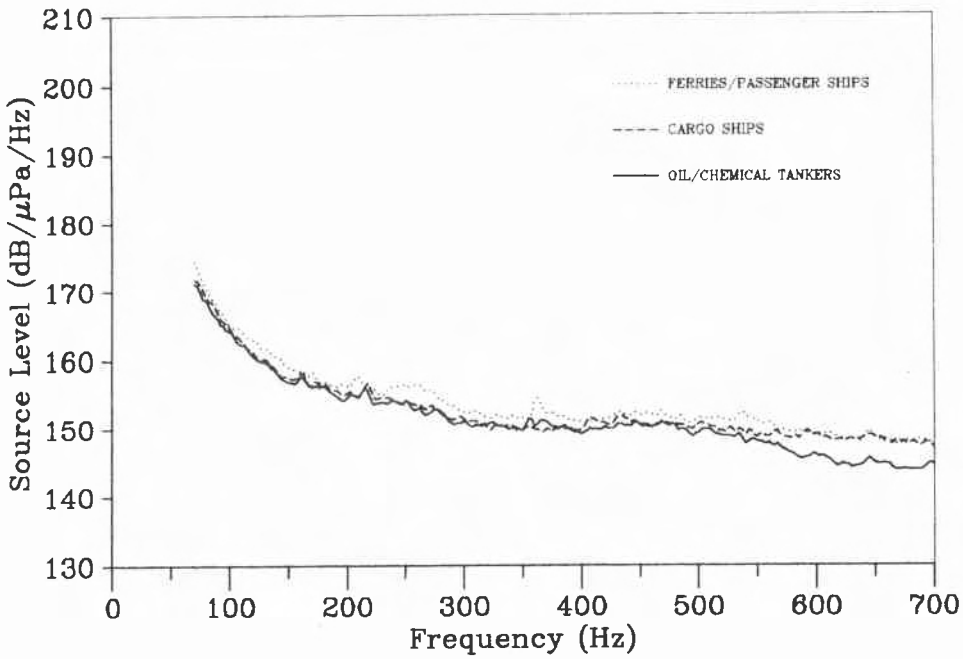

Fig. 9. The mean source spectra for the three ship classes.

ship classes are comparable. Furthermore, since the Genova sub-sample contains over 70% of the spectra in the full Genova sample, it is reasonable to conjecture that the source spectrum statistics for each ship class in the full Genova sample are comparable. If this is the case, the source spectrum statistics for any region should be largely independent of the particular mix of ship types in that region. Thus, to the extent that this is true, the source spectrum statistics of the preceding section should be applicable to other regions, provided that there are no important differences in the other ship characteristics for that region.

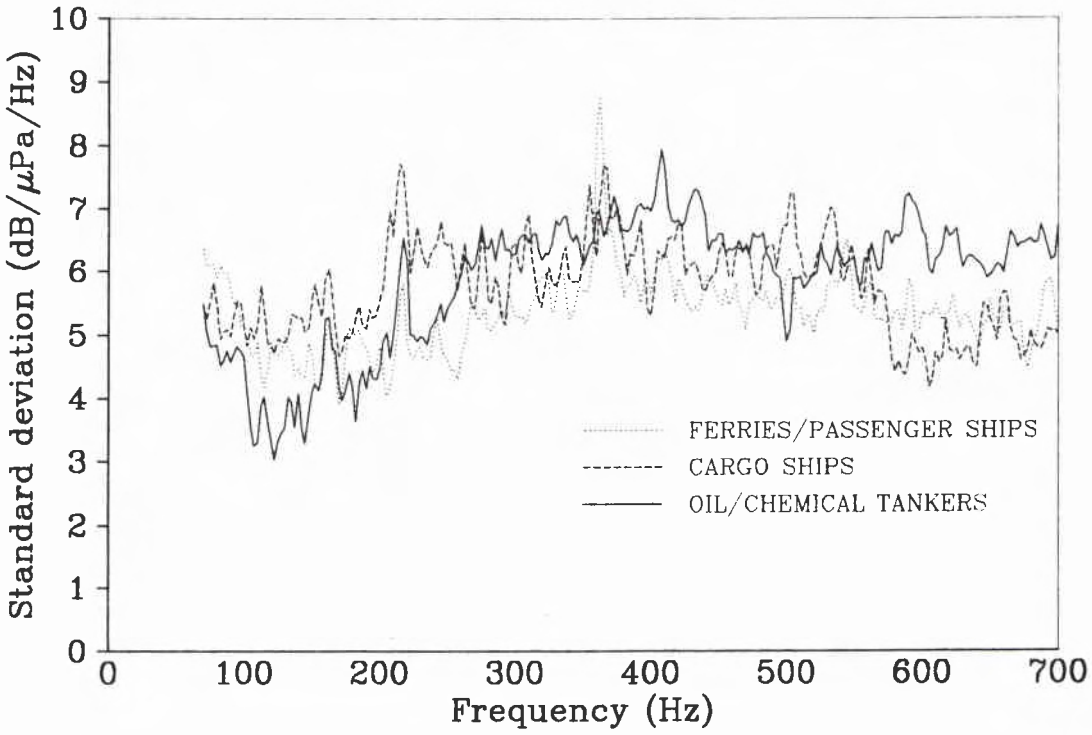

Fig. 10. **The standard deviation curves for the three ship classes.**

7. Summary and conclusions

This report describes a set of 50 source spectra obtained from merchant ships of opportunity near Genova, Italy. These spectra were obtained from radiated-noise spectra measured at the beamformer output of a towed array and a transmission-loss spectrum computed from a parabolic equation model. The ship characteristics were presented for the 32 spectra where the ship name was known. The sub-sample of 36 spectra with known ship type was characterized in terms of three ship classes – passenger/ferries, cargo ships and tankers. It was seen that the ship class percentages for this sub-sample differed significantly from the ship class percentages for either a Mediterranean population or a World population primarily because of the disproportionally large number of passenger/ferries in the Genova sub-sample.

The source-spectra were characterized in terms of the mean source spectrum and source-level histograms computed over three frequency bands. The mean spectrum was seen to be comparable in level and shape to a spectrum computed from the empirical model of Ross for a ship with four propeller blades and a propeller blade tip speed of 37.5 m/s. The source-level histograms for the low-frequency and the medium-frequency bands are approximately gaussian with standard deviations of 5 dB and 5.5 dB respectively. The histogram for the high-frequency band is skewed somewhat towards the low source-level values with a standard deviation of 6.8 dB. The increased spread in the high-frequency band is largely due to a greater variability in the shapes of the individual source spectra at the higher frequencies.

Finally, it was seen that the source spectra for the three ship classes have a comparable mean spectrum and a comparable standard deviation curve. From this result we conjecture that both the mean spectrum and the source-level histograms from the full Genova sample can be used as the source-spectrum statistics in noise models for other regions with different ship class percentages.

References

[1] GREENMAN, D., *ed.* Jane's Merchant Ships, 3rd edition, London, Jane's, 1987.

[2] Lloyd's Register of Shipping, Statistical Tables. London, 1982.

[3] ROSS, D. Mechanics of Underwater Noise, Oxford, UK, Pergamon Press, 1976.

[4] ODEGAARD, J. and THIELE, L. Underwater noise from the propellers, of a triple screw container ship, Report 82.54. Copenhagen, ODEGAARD DANNESKIOLD-SAMSOE K/S, 1983.

[5] COLOMBO, A., AUSONIO, P., GROSSI, L. and ACCARDO, L. Propeller induced noise and vibration reduction: acquired experience in design and testing approach. *In:* BUITEN, J. *ed.* Shipboard Acoustics. Proceedings of the 2nd international symposium on shipboard acoustics, ISSA'86, the Hague, the Netherlands, 7–9 October, 1986. Dordrecht, the Netherlands, Nijhoff, 1986: pp. 21–42.

[6] JENSEN, F.B. and MARTINELLI, M.G. The SACLANTCEN parabolic equation model (PAREQ). La Spezia, Italy, SACLANT Undersea Research Centre, 1985.

[7] ANGRISANO, G. and SEGRE, A.G. La carta batimetrica del Mediterraneo nord occidentale, I.I. 1501. Genova, Istituto Idrografico della Marina Italiana, 1969.

[8] SCRIPPS INSTITUTION OF OCEANOGRAPHY. Surface sediment distribution, Mediterranean Sea. San Diego, CA, 1970.

[9] JENSEN, F.B. and FERLA, M.C. SNAP: The SACLANTCEN normal-mode acoustic propagation model, SACLANTCEN SM-121. La Spezia, Italy, SACLANT Undersea Research Centre, 1979. [AD A 067 256]

intentionally blank page

Appendix A

An example of a noise surface time-series

The individual radiated-noise spectra $\mathrm{RL}_k(f)$ were obtained from the time series of frequency-angle noise surfaces. An example of a segment from one such time series is shown in Fig. A1. This segment consists of 12 consecutive surfaces each representing an 86 second average of the beam noise power. The beam steering angle, which is represented by the horizontal axis, increases non-linearly from $-90°$ at the left-hand-side of each surface to $+90°$ at the right-hand-side with -90 corresponding to forward endfire and $+90$ corresponding to aft endfire. The frequency, which is represented on the vertical axis, increases linearly from from 62.5 Hz at the bottom to 700 Hz at the top. The beam-noise levels for each surface are described in a relative scale by the color bar shown at the top of the figure. In the particular example shown here, the target-ship spectrum appears at different steering angles as time progresses. The spectrum is first seen weakly just aft of the broadside beam (surface 1). As time progresses, the received spectrum levels gradually increase and the steering angle gradually shifts towards the aft endfire beam. The level of the target spectrum can be seen to peak in surfaces 7, 8 and 9 before fading away in the last few surfaces.

The radiated-noise spectra $\mathrm{RL}_k(f)$ were obtained from the noise surfaces using a frequency-angle cursor to identify the steering angle with the maximum response in the target ship direction. After this angle had been identified in each surface, the beam number corresponding to this angle was recorded. These beam numbers were used in subsequent processing to extract the radiated-noise spectrum from the surfaces.

The complete time-series for a target could consist of as many as 20 noise surfaces acquired over a period of about 27 min. For many target ships, however, the radiated-noise spectra was well separated in angle from the noise spectra from other ships in as few as six of these surfaces.

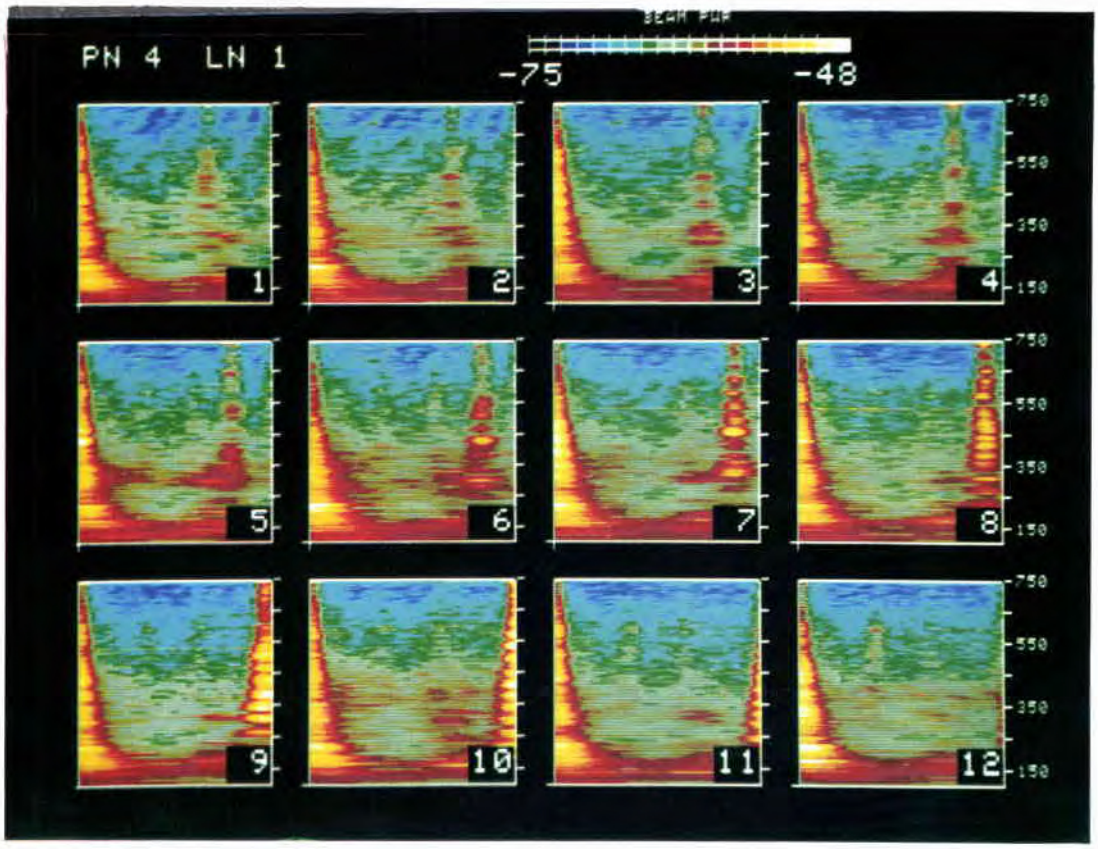

Fig. A1. A segment from a noise-surface time-series.

Appendix B

The transmission-loss computations

The transmission-loss spectra TL(f) were computed using the parabolic equation model PAREQ [6]. The bottom composition parameters required by this model were determined through the comparison with the measured transmission-loss data at 333 Hz over the full length of both tracks in Fig. 1 of Sect. 2. In addition, comparisons were made for a number of frequencies in a 100 Hz band about 333 Hz over selected range intervals. These comparisons were limited by the low signal-to-noise ratios at these frequencies. The parameters determined by this process were found to be representative of a coarse sand bottom with no overlying sediment layer. These parameters are

- Compressional bottom speed (C_{bottom}) of 1835 m/s.
- Relative bottom density ($\rho_{\mathrm{bottom}}/\rho_{\mathrm{water}}$) of 2.0.
- Compressional attenuation β_{c} of 0.7 dB/λ.

It should be noted that these parameters are not consistent with the bottom composition estimates available to us. These estimates, which were obtained by combining information from a number of survey charts for the region [7,8] are shown in Fig. B1 along with the approximate locations of the submarine canyons in the region.

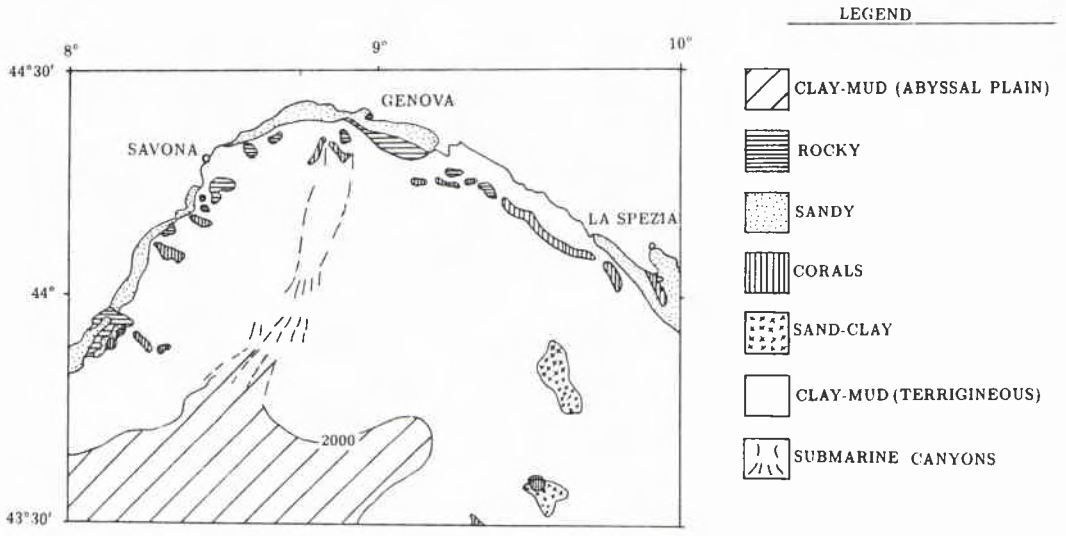

Fig. B1. Bottom composition estimates.

The transmission-loss functions $\mathrm{TL}(f, r)$ were obtained from 14 transmission-loss runs at frequencies ranging from 50.0 Hz to 700.0 Hz in 50.0 Hz steps. The transmission loss for the total set of 256 frequencies was computed from the individual runs through a linear interpolation in frequency. The range step for each run was 0.1 km and the total range interval was 0.0 to 30.0 km. To facilitate the range averaging used in the computation of the transmission-loss spectra, the transmission-loss functions were stored as 'transmission-loss matrices' $\mathrm{TL}(i, j)$, where i is the range index and j is the frequency index.

The six generic bottom profiles determined from the analysis of the tow-ship/target ship tracks are

(1) *Flat* (1000 m) from 0 to 35 km.

(2) *Flat* (1800 m) from 0 to 35 km.

(3) *Upsloping* (2000–800 m) from 0 to 30 km, then *flat* (800 m) to 35 km.

(4) *Downsloping* (800–2000 m) from 0 to 30 km, then *flat* (2000 m) to 35 km.

(5) *Downsloping* (1300–2000 m) from 0 to 25 km, then *flat* (2000 m) to 35 km.

(6) *Upsloping* (1600–1000 m) from 0 to 10 km, *downsloping* (1000–2000 m) from 10 to 30 km, then *flat* (2000 m) to 35 km.

The corresponding transmission-loss functions are shown Fig. B2. An independent check of the PAREQ results was made for the two range-independent profiles using the normal-mode model SNAP [9].

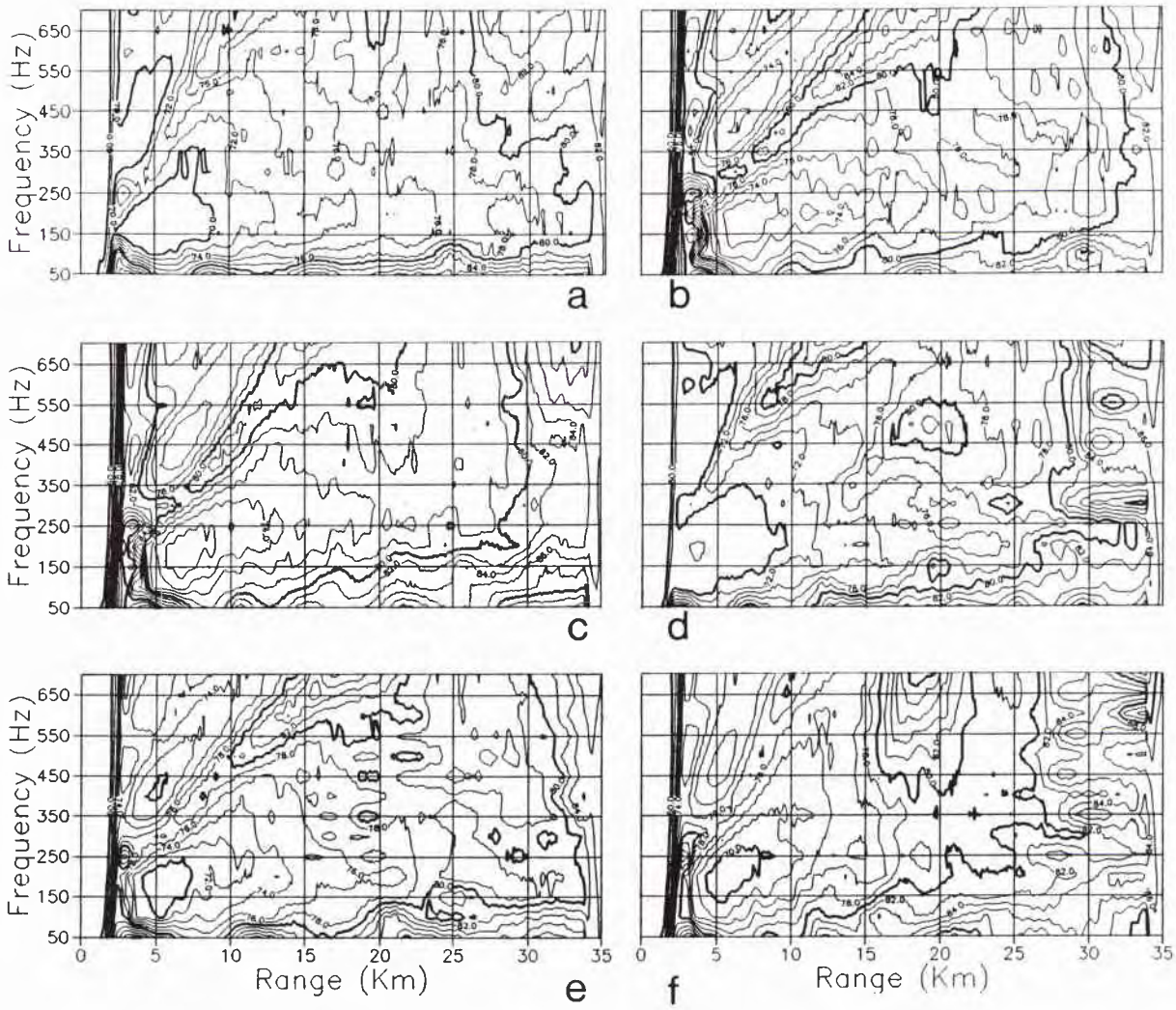

Fig. B2. **The six transmission-loss functions.**

Report no. changed (Mar 2006): SR-143-UU

Initial Distribution for SR-143

Ministries of Defence	
JSPHQ Belgium	2
DND Canada	10
CHOD Denmark	8
MOD France	8
MOD Germany	15
MOD Greece	11
MOD Italy	10
MOD Netherlands	12
CHOD Norway	10
MOD Portugal	2
MOD Spain	2
MOD Turkey	5
MOD UK	20
SECDEF US	68
NATO Authorities	
Defence Planning Committee	3
NAMILCOM	2
SACLANT	3
SACLANTREPEUR	1
CINCWESTLANT/ COMOCEANLANT	1
COMSTRIKFLTANT	1
CINCIBERLANT	1
CINCEASTLANT	1
COMSUBACLANT	1
COMMAIREASTLANT	1
SACEUR	2
CINCNORTH	1
CINCSOUTH	1
COMNAVSOUTH	1
COMSTRIKFORSOUTH	1
COMEDCENT	1
COMMARAIRMED	1
CINCHAN	3
SCNR for SACLANTCEN	
SCNR Belgium	1
SCNR Canada	1
SCNR Denmark	1
SCNR Germany	1
SCNR Greece	1
SCNR Italy	1
SCNR Netherlands	1
SCNR Norway	1
SCNR Portugal	1
SCNR Turkey	1
SCNR UK	1
SCNR US	2
French Delegate	1
SECGEN Rep. SCNR	1
NAMILCOM Rep. SCNR	1
National Liaison Officers	
NLO Canada	1
NLO Denmark	1
NLO Germany	1
NLO Italy	1
NLO UK	1
NLO US	1
NLR to SACLANT	
NLR Belgium	1
NLR Canada	1
NLR Denmark	1
NLR Germany	1
NLR Greece	1
NLR Italy	1
NLR Netherlands	1
NLR Norway	1
NLR Portugal	1
NLR Turkey	1
NLR UK	1
Total external distribution	250
SACLANTCEN Library	10
Stock	20
Total number of copies	280